

Phenomenology of Multipion Production in $\bar{p}p$ Annihilation Based on an Analysis of $\bar{p}p \rightarrow 5\pi$ at 3.25 GeV/c

R. Rajaraman and R. P. Jain

Department of Physics and Astrophysics, University of Delhi, Delhi-7, India

(Received 19 October 1970; revised manuscript received 28 December 1970)

We analyze some data for the reaction $\bar{p}p \rightarrow 2\pi^+2\pi^-\pi^0$ at 3.25 GeV/c. We study the dependence on different momentum-transfer variables, momentum distributions, and charge distributions. We compare the behavior with well-known characteristics of $\pi p \rightarrow$ nucleon + pions and $pp \rightarrow$ (2 nucleons) + pions. We also compare the data with computer-generated events constrained only by Lorentz-invariant phase space (LIPS). We find that the data agree in many respects with LIPS. Apart from a few statistically significant features mentioned in the text, the data show little dependence on the momenta or the charges. This is in sharp contrast with the pions produced in πp , Kp , or pp inelastic scattering. We discuss the result and its implications about annihilation processes and give arguments as to why our result might be valid at higher energies as well.

I. INTRODUCTION

An analysis of some data for the reaction $\bar{p}p \rightarrow 2\pi^+2\pi^-\pi^0$ from an experiment done at about 3.25 GeV/c by Ferbel *et al.*¹ is presented here.

Over the past few years, certain patterns appear to be emerging about the momentum distributions and the quantum-number distributions of the final-state particles in πp , pp , and to some extent, Kp inelastic processes. Our purpose here is to see if similar behavior is observed in baryon annihilation processes as well. We find that it is not. Instead, an alternative and simpler picture seems to be applicable to the products of $\bar{p}p$ annihilation.

Since our analysis is done with a view to contrasting $\bar{p}p$ annihilation with other multiparticle processes, we will first summarize the relevant features that characterize the latter before presenting our data.

In reactions such as $\pi p \rightarrow$ nucleons + pions or $pp \rightarrow$ (2 nucleons) + pions, as the energy increases the following broad features are now widely believed to emerge. First, in a majority of the events at least some, if not all, of the final particles seem to come out in the form of two "jets" or "clusters." The cluster may simply be one of the known resonances, or it may not. But its mass is small compared to the available energy \sqrt{s} in the c.m. frame². These two clusters essentially travel in near-forward and near-backward directions, respectively, in the over-all c.m. frame. The individual final particles seem to have relatively small transverse momenta,³ of the order of a few hundred MeV/c, even when the total lab energy increases to tens of GeV.

The total quantum numbers of the jets have also followed a pattern, whereby "vacuum" exchange processes are preferred.^{2,4,5} The preference for

such "diffractive dissociations" is not universal. [See the counterexample in the process $\pi^-p \rightarrow (2\pi^- \pi^+ \pi^0)p$ mentioned by Van Hove,⁶ where G parity is exchanged, and which is nevertheless dominant at 11 GeV/c.] But on the whole, diffractive dissociations are dominant, consistent with theoretical notions of the dominance of Pomeron exchange.

Finally, the clusters are produced peripherally. The "differential" cross section $d\sigma/dt$ (where \sqrt{t} is the momentum transfer from the incoming projectile to the forward cluster) is highly peaked at $t = t_{\min} \approx 0$, and may be roughly described by the form

$$d\sigma/dt \sim A e^{bt}.$$

While the slope b varies with the multiplicity and the individual reaction (see the work of Satz⁷ in this connection), it is of the order of the corresponding slope of the elastic πp or pp differential cross sections, and sometimes even higher. Conversely, it has been shown by one of the authors⁸ that if one assumes that a double-cluster production dominates with a $d\sigma/dt$ similar to the elastic shape, then this automatically leads to the observed small transverse momenta and also the observed insensitivity of the transverse momenta to large variations in the total energy.

Let us now consider $\bar{p}p$ reactions. They are naturally classified into two groups: (a) nonannihilation processes such as $\bar{p}p \rightarrow \bar{p}p +$ pions; (b) annihilation processes such as $\bar{p}p \rightarrow$ pions. These two groups are clearly quite different. Since group (a) allows the possibility of vacuum exchange, perhaps these also occur predominantly via diffractive dissociations and share the peripheral double-jet nature of the πp and pp inelastic collisions.⁹ On the other hand, the annihilation processes [group (b)],

of which our analysis is an example, may be expected to behave quite differently. Even if one divides the final particles into two clusters, the production of such clusters will require baryon exchange. Therefore these processes may be expected to decrease with increasing energy as some power of $1/s$, whether one uses Reggeon-exchange models or more general considerations, such as those of Feynman.¹⁰ There may also be significant differences in the charge and momentum distributions of the final particles, as compared to the double-jet configurations of the diffractive processes. For instance, it is quite conceivable that $\bar{p}p$ annihilation reactions take place for low impact parameters as compared to nonannihilation processes. In that case, the angular distribution of the final particles may be much more isotropic. This correlation between low impact parameters and isotropy is physically very clear in statistical models, as has been lucidly pointed out in Fermi's early work on the subject.¹¹

Our analysis of the $\bar{p}p \rightarrow 5\pi$ events indeed supports this conjecture. We find the following.

(a) Far from resembling a double-jet structure, the final pions are, to first approximation, isotropic in the c.m. frame, and seem to be governed largely by Lorentz-invariant phase space (LIPS) alone, with an effective constant matrix element. We show this by comparing our data with computer-generated events programmed to satisfy only LIPS and energy-momentum conservation.

(b) There is no pronounced preference for any given charge configuration.

(c) There is no sharp dependence on any four-momentum transfer. This is in contrast to the strongly peaked $d\sigma/dt$ for diffractive processes.

In Sec. III we will discuss the possible implications of our findings and their relationship to resonance production, Regge-exchange mechanisms, etc. Let us now present the details of the analysis.

II. ANALYSIS OF DATA

We had at our disposal about 970 events of the reaction $\bar{p}p \rightarrow 2\pi^+2\pi^-\pi^0$, at a lab momentum of about 3.25 GeV/c. We also use, for purposes of comparison, a sample of about 1000 events generated by a computer. These computer-generated data, which we will call "random data," were programmed to simulate events constrained *only* by LIPS and total energy-momentum conservation, the total energy being the *same* as that of the real data. The reason for using the random data was obviously because of the difficulties in getting analytic expressions for the five-particle phase space. With these two sets of real data and random data, the following analysis was done. All the

data and the analysis refer to the c.m. frame.

Dependence on Momentum Transfer

We first divided the five pions in each event of the data into two groups based on the *sign* of the c.m. longitudinal momentum p_z . The corresponding momentum transfer squared, t , can be defined for each event as $t = (k_1 - \sum_{\text{forward}} p_i)^2$, where k_1 is the four-momentum of the antiproton [Fig. 1(a)], and $\sum_{\text{forward}} p_i$ is the sum of the momenta of the pions having positive p_z . A plot of $d\sigma/dt$ with respect to t is given in Fig. 2. Figure 2 has two curves, corresponding to the real and the random data, respectively. The real-data curve in Fig. 2 may be roughly fitted with the exponential form e^{bt} , where $b \approx 2 \text{ GeV}^{-2}$. Even this modest peak is mostly owing to the kinematics of five-particle phase space,¹² as evidenced by the near overlap with the corresponding curve for the random data.

This is to be contrasted with a double-jet structure, where the dependence on precisely this momentum transfer would be much more steep. Thus, in diffractive-dissociation processes, b is of the order of 6–10 GeV^{-2} or greater.^{3,7} The absence of such a sharp peak in our data, and the similarity between the two curves in Fig. 2, are a strong indication of the absence of quasi-two-body final state, or a double-jet structure. Instead, the five pions seem to be coming out isotropically, constrained mostly by phase space.

Next we checked whether there was a stronger dependence on any other momentum-transfer variable. For this, we included the least-backward (least $|p_z|$) pion from the backward cluster in the "forward" cluster and calculated the new momentum transfer squared t' . Figure 1(a) clarifies what we did and what t' is.

Similarly the variable t'' corresponds to shifting the least-forward (least $|p_z|$) particle from the forward cluster to the backward one. We plot $d\sigma/dt'$ and $d\sigma/dt''$ in Fig. 3(a). Since the problem is completely symmetrical between the forward and back-

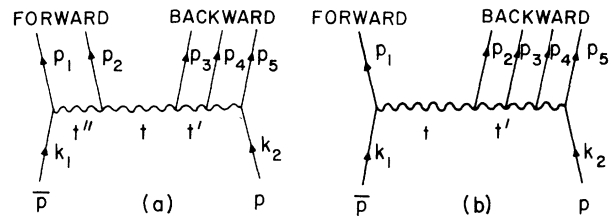


FIG. 1. Diagrams showing $\bar{p}p \rightarrow 5$ pions. (a) Example of a 2-3 split, i.e., two pions having one sign of p and three pions having the other sign. (b) Example of a 1-4 split.

ward directions (except for an over-all change of the sign of the charge), one expects $d\sigma/dt'$ and $d\sigma/dt''$ to be identical. That this is so is clear from Fig. 3(a), where the triangles correspond to $d\sigma/dt'$ and the circles to $d\sigma/dt''$.

It is clear that $d\sigma/dt'$ is even less sharply peaked than the $d\sigma/dt$ of Fig. 2. Thus, there is no pronounced "peripherality" with respect to either t' or t'' . Instead, the curve in Fig. 3(a) agrees well with the corresponding curve in Fig. 3(b) for the random data, indicating once again the resemblance of the real data with purely phase-space governed isotropy.

We now mention the anomalous δ -function peaks in Figs. 3(a) and 3(b) at $t = +M^2 = 0.88 \text{ GeV}^2$. These correspond to cases where one pion has one sign for p_z and the other four have the opposite sign. In such cases either t' or t'' defined above equals $(k_1 - 0)^2 = k_1^2 = M^2$. We note that the spike has approximately the same height in Figs. 3(a) and 3(b). Thus, even in the ratio of events with 1-1-vs-2-3 splits in the sign of p_z , the real and random data agree.

Longitudinal Momentum Distribution

Figure 4 gives a plot of the p_z distribution of the pions for the real and random data where we have included pions of all charge in the real data. The

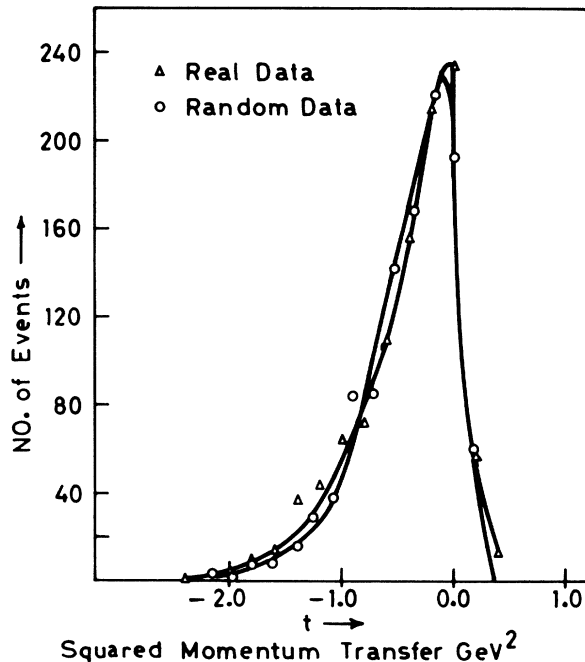


FIG. 2. Comparative curves of $d\sigma/dt$ for the actual data (triangular points) and the random (LIPS) data (circular points).

strong resemblance between the behavior of the two sets of points is evident – so much so that it was not fruitful to draw two curves.

Angular Distribution

In view of the emerging similarity between the real data and the isotropic random data, we attempted a more direct test of isotropy by plotting each pion in the real data as a point on the (p_x, p_z) plane. Note that we are talking about spin-averaged data where axial symmetry about the z axis can be assumed. To check the angular distribution in the (p_x, p_z) plane, we divided it into 12 sectors of 30° each and counted the points in each sector. These counts are given in Fig. 5. Figure 5(a) gives the total number of pions (including all three charges) in each sector. This count is for pions

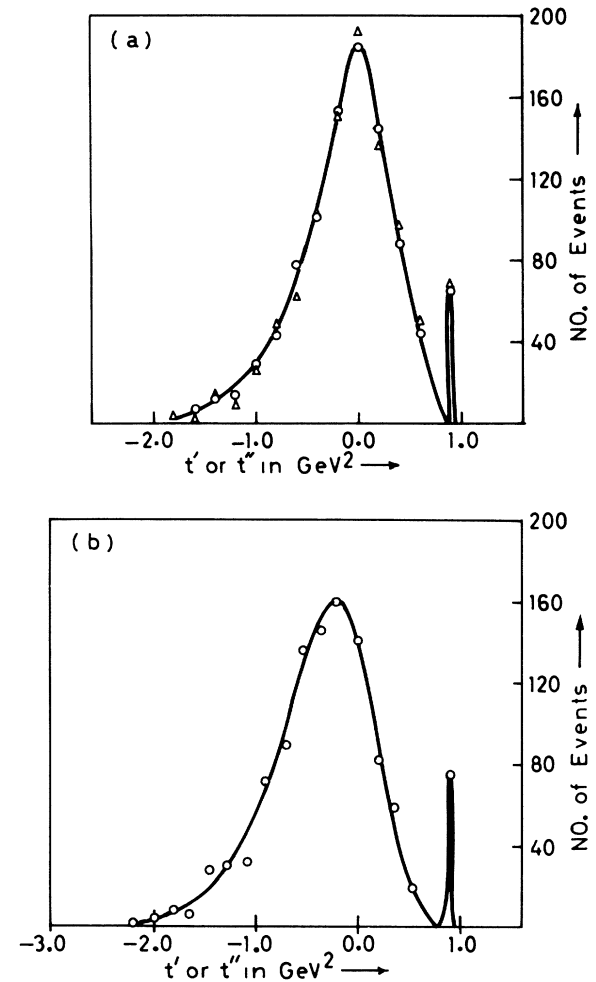
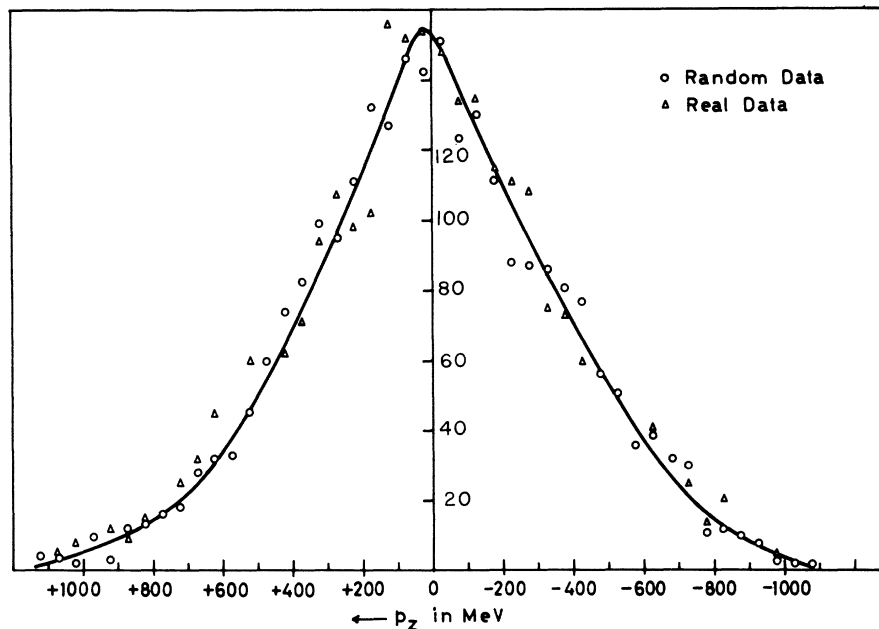


FIG. 3. Curves for $d\sigma/dt' = d\sigma/dt''$ for the real data (a) and the random (LIPS) data (b). The spikes at $t = M^2$ in both curves are explained in the text.

FIG. 4. Longitudinal-momentum distributions in the c.m. frame for the real and the random data. The triangular points give the real data and the circular points the random data. The curves are drawn only to guide the eye.



with momentum $|\vec{p}|c \leq 5m_\pi c^2$, which constitute more than 80% of all the pions in the real data. One can see that the distribution is in good agreement with isotropy. A calculation of

$$\chi^2 = \sum_{i=1}^{12} \frac{(n_i - \bar{n})^2}{\bar{n}},$$

where n_i is the number of points in a given sector and $\bar{n} = \frac{1}{12}N$ is the number of points expected from isotropy, yields a value $\chi^2 = 6.1$. This is low considering that in a counting experiment with 12 bins, one would on the average expect $\chi^2 \approx 12$ since $(n_i - \bar{n}) \sim \sqrt{\bar{n}}$ because of statistical fluctuations.

Figures 5(b), 5(c), and 5(d) give the separate counts for π^+ , π^- , and π^0 , which are each consistent with isotropy. The χ^2 of these three distributions are 14.6, 6.1, and 12, respectively, when fitted to isotropy. The above statements are for the majority (80%) of the outgoing points whose $|\vec{p}| \leq 5m_\pi c$. If one includes all the pions, then, as seen in Fig. 5(e), the isotropy is somewhat removed. There is a small but systematic preference for forward and backward directions. This is reminiscent of what happens in a double-jet distribution, although nowhere nearly as pronounced. Since the deviation from isotropy comes from the addition of the high-energy pions, it is possible that these are emitted singly by the incoming proton or antiproton before the annihilation takes place.

Invariant-Mass Plot

In Fig. 6, we have shown the invariant-mass distribution of the forward cluster. By symmetry, the

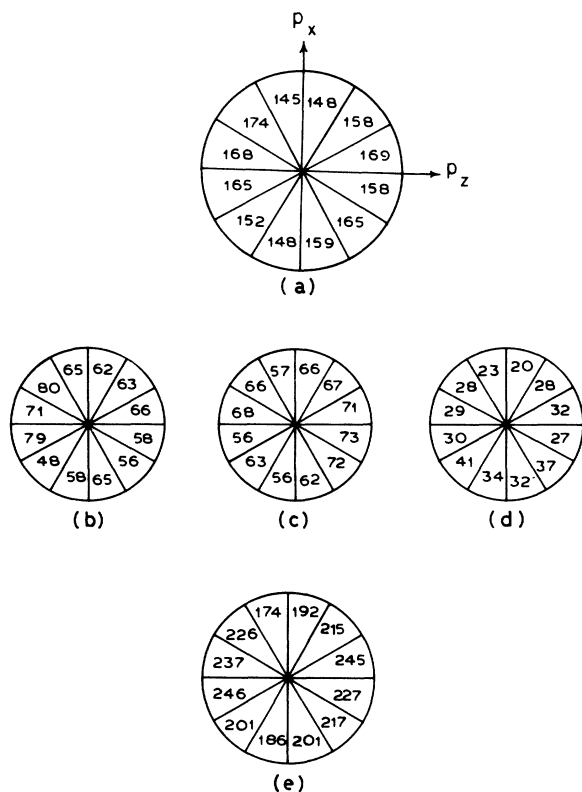


FIG. 5. Number distribution in 12 equally divided (30°) sectors in the (p_x, p_z) plane. (a) Pions with momentum $|p_z| \leq 5m_\pi c$. These are over 80% of all pions. (b), (c), and (d) Separate distributions for π^+ , π^- , and π^0 , respectively. (e) Count for all pions regardless of energy. In all cases, the horizontal axis is the z axis.

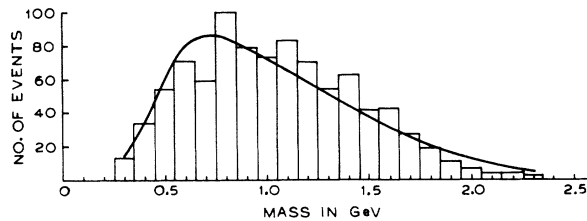


FIG. 6. Invariant-mass plot for the forward cluster. The histograms correspond to the actual data and the curve to LIPS.

backward cluster should have a similar distribution. For comparison the corresponding curve for LIPS is exhibited. The data do show some structure, in the form of a mild peak in the 750–850-MeV region, which could well be due to ρ and ω . Apart from this, there is good agreement with the LIPS curve.

We also show the $\pi^+\pi^0$ invariant-mass distribution in Fig. 7. There is a broad peak in the 650–900-MeV region, once again indicating some ρ production. But the peak is not anywhere nearly as strong as in, say, $\gamma p \rightarrow p\pi^+\pi^-$.

Charge Distributions

As mentioned in the Introduction, processes such as $\pi p \rightarrow \pi p +$ pions show a preference for diffractive dissociation. The forward cluster tends to have the same quantum numbers as the incoming projectile, and the backward cluster those of the target. This is evidenced, for example, in the Van Hove plots.⁵ We find that there is no corresponding preference in $\bar{p}p \rightarrow 2\pi^+2\pi^-\pi^0$ in terms of the charge configurations of the forward-vs-backward particles.

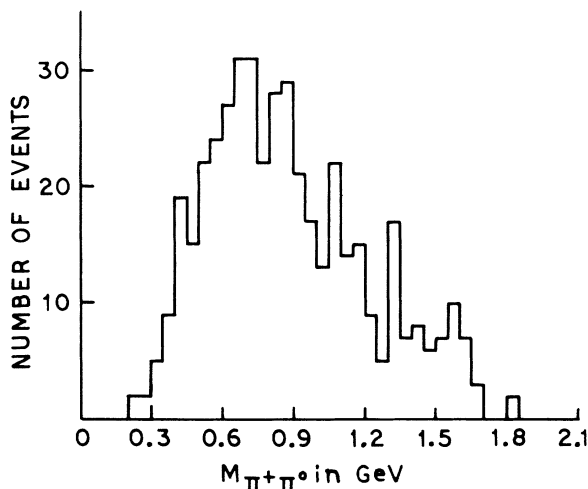


FIG. 7. Invariant-mass plot of the $\pi^+\pi^0$ system.

Clearly our data have two types of events – the majority with a 2-3 split in the sign of p_z , and a minority with a 1-4 split. These two categories cannot be easily compared with each other since they would carry different statistical weights because of phase space. But the different charge configurations within the 2-3 split events can be compared with each other since their kinematic conditions are the same. Such a comparison is given in Table I. Column 5 gives the subtotals for a given partition, e.g., $\pi^+\pi^0$, $\pi^+\pi^-\pi^-$. Since in $2\pi^+2\pi^-\pi^0$ there are four ways of forming $\pi^+\pi^-$, two ways each of forming $\pi^+\pi^0$ or $\pi^-\pi^0$, and only one way of forming $\pi^+\pi^+$ or $\pi^-\pi^-$, these subtotals have to be suitably normalized as in column 6, before comparison. All these normalized subtotals can be seen to lie between 41 and 51. Thus, to first approximation, the data are consistent with random charge configurations. The approximate randomness of the data in momentum space observed in Figs. 2–5 appears to be accompanied by a similar randomness in charge space.

III. CONCLUSIONS

In summary, our data seem to show a very simple pattern: The matrix element, to first approximation, shows little dependence on the momenta or the charge of the pions, with LIPS and energy-momentum conservation being the only constraints. It is tempting to make the generalization that the results of our particular analysis are valid for all high-energy baryon-annihilation processes. Such a generalization can certainly be questioned at face value. Even in our own data, the resemblance with the computer-generated random LIPS data is still not exact. There is a slight preference [Fig. 5(e)] for the pions to lie in forward and backward cones in momentum space. Further, there is a certain amount of anisotropy in charge configurations as well. Thus, within the partition ($\pi^+\pi^+$, $\pi^-\pi^-\pi^0$), the $\pi^+\pi^+$ pair prefers to come out backward, i.e., in the direction of the proton [see rows 4(a) and 4(b) in Table I], although the five different partitions in column 6 are nearly equally populated.

It is possible that these tendencies towards asymmetry will become more pronounced at higher energies. However, a recent analysis of $\bar{p}p \rightarrow$ pions at 6.94 GeV/c by Bar-Nir *et al.*¹³ shows that the pions, at their typical multiplicity, are consistent with isotropy. Further, one must remember that the asymptotic region sets in much earlier in $\bar{p}p \rightarrow$ pions owing to the absence of final-state nucleons. Thus, the 6.94-GeV/c ($s \approx 13\text{-GeV}^2$) data of Bar-Nir *et al.* for $\bar{p}p \rightarrow$ pions should be compared to $pp \rightarrow pp +$ pions at $s \approx 31\text{ GeV}^2$ or $p_{\text{lab}} \approx 15.4\text{ GeV}/c$ in order

TABLE I. Relative abundance of different charge configurations in events with a 2-3 split with respect to p_z . The difference between columns 5 and 6 is explained in the text.

1	2	3	4	5	6
Serial No.	Positive- p_z particles	Negative- p_z particles	No. of events	Subtotals	Normalized subtotals
1(a)	$\pi^+\pi^-$	$\pi^+\pi^-\pi^0$	93		
1(b)	$\pi^+\pi^-\pi^0$	$\pi^+\pi^-$	94	187	46.75
2(a)	$\pi^+\pi^0$	$\pi^+\pi^-\pi^-$	35		
2(b)	$\pi^+\pi^-\pi^-$	$\pi^+\pi^0$	57	92	46
3(a)	$\pi^-\pi^0$	$\pi^+\pi^+\pi^-$	42		
3(b)	$\pi^+\pi^+\pi^-$	$\pi^-\pi^0$	41	83	41.5
4(a)	$\pi^+\pi^+$	$\pi^-\pi^-\pi^0$	18		
4(b)	$\pi^-\pi^-\pi^0$	$\pi^+\pi^+$	29	47	47
5(a)	$\pi^-\pi^-$	$\pi^+\pi^+\pi^0$	29		
5(b)	$\pi^+\pi^+\pi^0$	$\pi^-\pi^-$	22	51	51

for the pions to have the same available energy. The data for $\pi p \rightarrow \pi p +$ pions at 16 GeV/c certainly show strong asymmetry,⁵ so that the lack of similar asymmetry in our data, supported by the work of Bar-Nir *et al.*, is significant.

It is therefore not out of order to speculate that in high-energy annihilation processes, the matrix element to first approximation is a constant.¹⁴ If this is so, it would be a great simplification, both phenomenologically and for theoretical calculations such as the shadow effect of annihilation processes on $\bar{p}p$ elastic scattering.⁹

Lastly, we do not imply that the conventional mechanisms of hadron physics, such as formation of resonances, or Reggeon exchange mechanisms, are absent here. In all likelihood, the final pions often come out as ρ or ω mesons which subsequently decay (see Figs. 6 and 7). It is also possible that these are produced via single-Regge or multi-Regge mechanisms. We are only saying that in the multipion system, the correlations due to these individual mechanisms get washed out.¹⁴ Indeed, as the mean multiplicity increases with energy, it is increasingly cumbersome (and hence of decreasing

usefulness) to analyze the phenomena in terms of resonances. It may be more useful to look for statistical features as we have tried to do here. In conclusion then, we conjecture that the following simple picture is useful as an approximation for $\bar{p}p$ scattering.

When the $\bar{p}p$ collision occurs at low impact parameters, annihilation takes place, producing mesons (mostly pions) which can be treated statistically. They correspond to low total angular momentum and very large temperatures, i.e., they are purely phase-space governed.

When the $\bar{p}p$ collision occurs at larger impact parameters, the dominant process is presumably nonannihilational, viz., $\bar{p}p \rightarrow \bar{p}p +$ (pions and kaons). These may well be diffractive and anisotropic.

ACKNOWLEDGMENTS

This work would not have been possible but for the continued generosity of Professor T. Ferbel and his collaborators, Dr. D. Cohen and Dr. R. Holmes, who provided all the raw data and some computational help. We are very grateful to them.

¹T. Ferbel *et al.*, Phys. Rev. **137**, B1250 (1965). Although this experiment and several interesting features, such as the partial cross sections for different channels, etc., were reported in this paper, the detailed final-state analysis of the raw data was not. Our motivation for undertaking the latter is given in the text.

²G. Cocconi, Phys. Rev. **111**, 1699 (1958); R. K. Adair, *ibid.* **172**, 1370 (1968).

³The smallness of the transverse momenta has been observed both in accelerator data [e.g., R. Honecker *et al.*, Nucl. Phys. **B13**, 571 (1969)] and in cosmic-ray data [e.g., J. F. de Beer *et al.*, Can. J. Phys. **46**, 737 (1968)].

⁴M. L. Good and W. D. Walker, Phys. Rev. **120**, 1857 (1960); T. T. Chou and C. N. Yang, *ibid.* **175**, 1832 (1968),

and experimental references therein.

⁵A. Bialas *et al.*, Nucl. Phys. **B11**, 479 (1969); J. Bartsch *et al.*, *ibid.* **B19**, 381 (1970).

⁶L. Van Hove, CERN Report No. CERN-TH-1209, 1970 (unpublished).

⁷H. Satz, Phys. Letters **32B**, 380 (1970).

⁸R. Rajaraman, Phys. Rev. D **1**, 118 (1970).

⁹The separation of $\bar{p}p$ reactions into these two classes and the similarity of the nonannihilational process to corresponding pp inelastic processes is very reasonable. See, for instance, J.-J. J. Kokkedee, Nuovo Cimento **43**, 919 (1966); and R. Henzi, A. Kotanski, D. Morgan, and L. Van Hove, Nucl. Phys. **B16**, 1 (1970).

¹⁰R. P. Feynman, Phys. Rev. Letters **23**, 1415 (1969).

¹¹E. Fermi, Phys. Rev. 81, 683 (1951).

¹²We are using the metric $\overline{p}^2 = E^2 - |\vec{p}|^2$, so that the momentum transfer squared, t , is usually negative. However, in our case, since the outgoing pions have a smaller mass than the incoming nucleons, small positive values of $t \leq (M - m_\pi)^2$ are possible. Hence the tail in Fig. 2 for $t > 0$. However, the vast majority of events have $t < 0$, and we are primarily concerned with the shape of the curve in this region.

¹³I. Bar-Nir *et al.*, Nucl. Phys. B20, 45 (1970).

¹⁴The isotropy may well break down if the channel considered has many fewer pions than the mean multiplicity at that energy. Thus we would not suggest that there will be isotropy for $\bar{p}p \rightarrow 3\pi$ (say) at high energies. We believe that the isotropy arises because of the averaging out of detailed structure, and will hold for the dominant channels where the multiplicity is close to the average multiplicity.